On the Analysis of Dielectric Relaxation Data of Poly(ether ether ketone)

A. A. Goodwin* and G. P. Simon

Department of Materials Engineering, Monash University, Clayton, Victoria 3168, Australia

Received February 22, 1995
Revised Manuscript Received June 14, 1995

Introduction

Poly(ether ether ketone) (PEEK) is a high-performance thermoplastic in which rigid aromatic groups are separated by flexible ether linkages and stiff ketone linkages in a fully para-aromatic chain structure. This structure confers upon PEEK a high glass transition temperature and high melting point, excellent mechanical properties, thermal stability, and solvent resistance.[1] The study of PEEK has contributed to a greater understanding of structure/property relationships in polymers as it can be obtained in a fully amorphous state, or with a range of crystallinities, whose morphology depends upon the processing history. The fine detail of how the polymer chains are arranged in the crystalline and amorphous regions of PEEK continues to be an area of active research. The existence of a "rigid amorphous phase" (RAP) has been postulated to exist in a number of semicrystalline polymers,[2-4] including PEEK, where those amorphous chains which are in close proximity to crystalline regions are constrained and are only able to relax at temperatures above the glass transition. Experimental investigations of the rigid amorphous phase in PEEK have been carried out using differential scanning calorimetry,[5] dynamic mechanical analysis,[6] and dielectric relaxation spectroscopy[7,8] (DRS). The essential parameter for quantifying the rigid amorphous phase using DRS is the relaxation strength $\Delta\epsilon = \epsilon_0 - \epsilon_\infty$, where ϵ_0 and ϵ_∞ are the relaxed and unrelaxed permittivities, respectively. This method involves a comparison of $\Delta\epsilon$ of amorphous and semicrystalline samples as a function of temperature to demonstrate that increasing numbers of dipoles only begin to relax above the glass transition temperature, as the RAP becomes mobile. For comparative purposes the amorphous relaxation strength must be *extrapolated* to higher temperatures, at which crystallization would usually occur, to give an estimate of the temperature dependence. This can result in uncertainty in the value of the RAP. The strength of a particular relaxation process can be established from the fitting of common empirical relaxation functions to dielectric data measured in the frequency domain, usually represented in the form of Cole–Cole or loss/frequency plots.

In this work we report on the dielectric α-relaxation behavior of amorphous PEEK and the determination of the relaxation strength, and associated parameters, using nonlinear curve fitting.

Experimental Section

Materials. Thin sheets (<1 mm) of amorphous PEEK (grade 381G supplied by ICI, Australia) were prepared by compression molding of dry granules at 400 °C followed by quenching into ice/water.

Dielectric Measurements. Dielectric data were obtained using a Gen Rad 1689 Digibridge interfaced to a Hewlett-Packard computer over the frequency range 15–10^5 Hz. PEEK samples, 17 mm in diameter, were prepared for analysis by vacuum sputtering gold onto both polymer surfaces to ensure good electrical contact with the cell electrodes. The dielectric cells were three-terminal guarded, and samples were equilibrated for some minutes in a Labmaster oven prior to data collection. All data were obtained in an isothermal mode, as a function of frequency at constant temperature, and the main variable determined was the dielectric loss, ϵ''. The temperature range for isothermal measurements of the dielectric loss was 151–154 °C, the lower limit being enforced by the low-frequency limit of the dielectric bridge and the upper limit chosen so as to ensure that the sample remained amorphous throughout data collection. PEEK crystallizes rapidly at temperatures above T_g, and it is this feature which restricts dielectric measurements to a narrow temperature range.

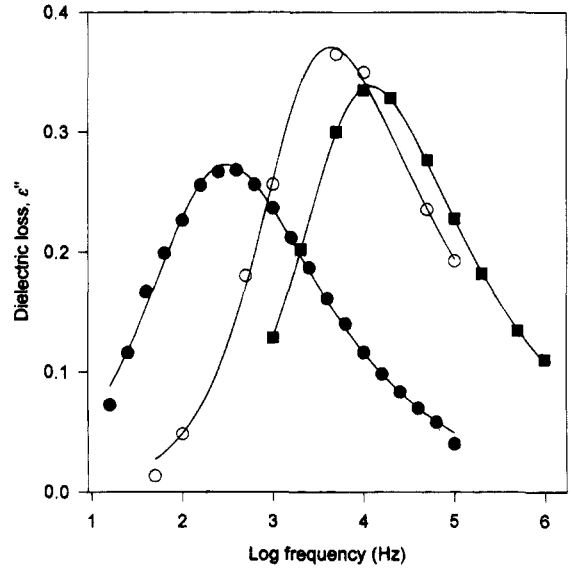

Figure 1. Dielectric loss curves for PEEK: (●) this study at 154 °C; (○) ref 8 at 158 °C; (■) ref 7 at 164 °C. Solid lines are curve fits to the Havriliak–Negami equation.

Curve Fitting. Nonlinear least-squares curve fitting was accomplished by use of the commercial PeakFit software (Jandel Scientific) which uses the iterative Marquardt–Levenberg fitting algorithm. This involves estimating values for the adjustable parameters such that the function

$$\chi^2 = \sum_{i=0}^{n}\left[\frac{f(x_i) - y_i}{\sigma_i}\right]^2$$

where $y = f(x)$, with f representing a model fitting function, and σ is standard deviation, is minimized. This procedure provides values for the adjustable parameters such that the fitting function is optimum in a least-squares sense. A fit is converged when χ^2 is unchanged within the eighth significant figure for five full iterations. The confidence intervals for the model parameters are determined at the 95% limit using a method outlined by Draper and Smith.[9]

A graphical prefitting method was used to manipulate the fitting function on the screen to match the experimental data as closely as possible prior to fitting.

Experimental Results

The frequency dependence of the dielectric loss for amorphous PEEK at 154 °C is shown in Figure 1. Also included in the figure are data abstracted from two recently published studies on the rigid amorphous fraction in PEEK, by Huo and Cebe[7] and Kalika and Krishnaswamy.[8] The data in these references were obtained from isochronal measurements, with the sample being heated at a constant rate. All plots show an asymmetric broadening, or skew, on the high-frequency side, which is a typical, although relatively unexplained, feature of the dielectric response of amorphous poly-

0024-9297/95/2228-7022$09.00/0

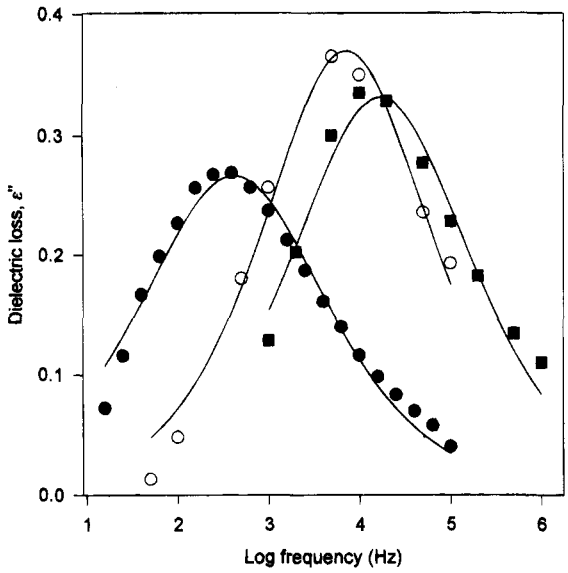

Figure 2. Dielectric loss curves for PEEK: (●) this study at 154 °C; (○) ref 8 at 158 °C; (■) ref 7 at 164 °C. Solid lines are curve fits to the Cole–Cole equation.

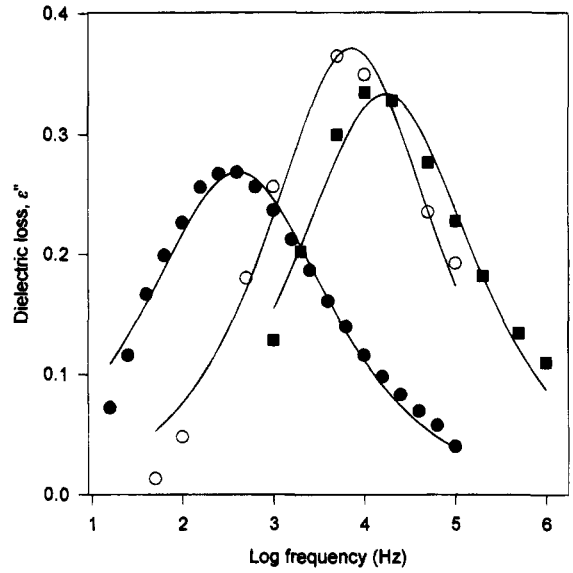

Figure 3. Dielectric loss curves for PEEK: (●) this study at 154 °C; (○) ref 8 at 158 °C: (■) ref 7 at 164 °C. Solid lines are curve fits to the Fuoss–Kirkwood equation.

mers. There are significant differences in the maximum values of ϵ'' which may be related to the bridge calibration, the electrode–sample interface, and the morphology and grade of PEEK used. The shifts in peak position reflect the different measurement temperatures at which the data are plotted. It is well-known that dielectric data in this form can be fitted to a number of empirical expressions, and, in this study, we compare the results from the fitting of the Fuoss–Kirkwood (FK), Cole–Cole (CC), and Havrilik–Negami (HN) functions to experimental PEEK data.

The Fuoss–Kirkwood[10] expression is given by

$$\epsilon''(\omega) = \frac{\epsilon_0 - \epsilon_\infty}{2}\beta_{fk} \operatorname{sec} h\beta_{fk} \ln \omega\tau_{fk} \qquad (1)$$

where ϵ_0 and ϵ_∞ are the relaxed and unrelaxed permittivities, respectively, β_{fk} is a symmetrical broadening parameter which assumes no skew, and τ_{fk} is a characteristic relaxation time.

The Cole–Cole[11] expression is

$$\frac{\epsilon^*(\omega) - \epsilon_\infty}{\epsilon_0 - \epsilon_\infty} = \frac{1}{1 + (i\omega\tau_{cc})^{\beta_{cc}}} \qquad (2)$$

where β_{cc} characterizes symmetrical broadening. When β_{cc} is equal to 1, a simple Debye process is implied.

The Havriliak–Negami[12] expression is given by

$$\frac{\epsilon^*(\omega) - \epsilon_\infty}{\epsilon_0 - \epsilon_\infty} = \frac{1}{[1 + (i\omega\tau_{hn})^{\beta_{hn}}]^{\alpha_{hn}}} \qquad (3)$$

α_{hn} and β_{hn} characterize the skew and broadness, respectively, of the isothermal loss peaks.

The loss curves in Figure 1 are well fitted by the HN expression at both low and high frequencies, as shown by the solid lines. The same data are then plotted in Figures 2 and 3 and fitted to the CC and FK expressions, also shown as solid lines. Here the symmetrical curve fits are quite clearly less satisfactory and are unable to account for the high-frequency skew. The different curve fits are compared in Figure 4 which shows the dielectric loss curve for PEEK at 158 °C taken from ref 8. There is a significant shift to higher

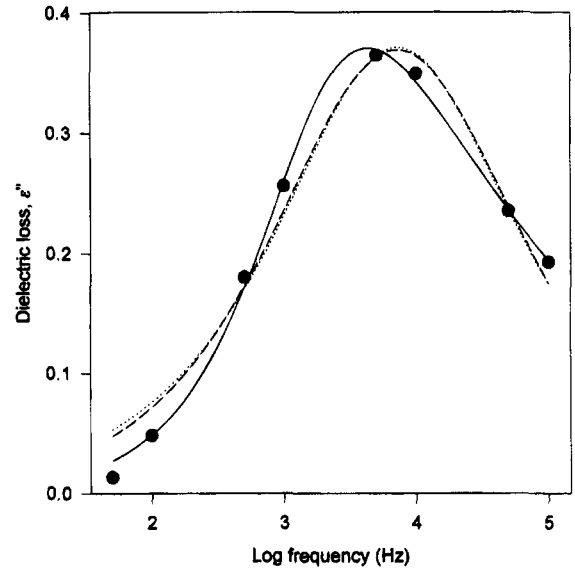

Figure 4. Dielectric loss curves for PEEK at 158 °C abstracted from ref 8: (···) fit to the Fuoss–Kirkwood equation; (- - -) fit to the Cole–Cole equation; (—) fit to the Havriliak–Negami equation.

frequencies of the maximum in dielectric loss, ϵ''_{max}, when the CC and FK functions are employed. These two functions produce fitted curves that are almost identical except at low frequencies where the curves begin to diverge. The dielectric parameters derived from curve fitting and the associated errors are listed in Table 1. The fitted parameters for the data of Kalika and Krishnaswamy[8] at 150 and 152 °C and of Huo and Cebe[7] at 155 and 158 °C are subject to large errors which result from only a limited part of the loss curve appearing within the frequency window at these temperatures.

CC and FK Analysis. The values of relaxation strength and relaxation time derived from the fitting of the CC equation to experimental data are identical to the corresponding values determined by the FK equation, across all three data sets. The relaxation strength decreases with increasing temperature in all cases and is similar in value to that determined by fits to Cole–Cole plots in ref 7 and 8. Values of the

Table 1. Fuoss–Kirkwood, Cole–Cole, and Havriliak–Negami Fits to PEEK Data[a]

(a) Fuoss–Kirkwood Fits to PEEK Data[a]

sample	T (°C)	$\Delta\epsilon$	β_{fk}	log τ(s)	$\chi^2 \times 10^3$	MSEE $\times 10^3$
this study	151	1.40 ± 0.02	0.42 ± 0.01	−2.58 ± 0.02	0.30	4.29
this study	153	1.27 ± 0.02	0.45 ± 0.01	−3.07 ± 0.02	1.43	9.18
this study	154	1.12 ± 0.03	0.48 ± 0.02	−3.41 ± 0.02	2.67	12.5
ref 8	150	1.92 ± 0.14	0.39 ± 0.03	−2.64 ± 0.10	0.84	12.7
ref 8	152	1.45 ± 0.06	0.53 ± 0.03	−3.32 ± 0.03	1.48	17.2
ref 8	154	1.23 ± 0.07	0.54 ± 0.04	−3.89 ± 0.05	2.35	21.7
ref 8	156	1.36 ± 0.16	0.57 ± 0.10	−4.19 ± 0.09	1.62	56.9
ref 8	158	1.40 ± 0.08	0.53 ± 0.04	−4.66 ± 0.03	3.67	27.1
ref 8	160	1.23 ± 0.05	0.60 ± 0.03	−5.03 ± 0.03	1.21	15.6
ref 7	155	3.86 ± 5.01	0.32 ± 0.03	−1.80 ± 0.75	0.50	8.49
ref 7	158	1.96 ± 0.13	0.36 ± 0.01	−3.56 ± 0.09	0.30	6.51
ref 7	161	1.54 ± 0.05	0.43 ± 0.02	−4.46 ± 0.03	0.80	10.7
ref 7	164	1.35 ± 0.06	0.49 ± 0.03	−5.03 ± 0.04	2.25	17.9

(b) Cole–Cole Fits to PEEK Data

sample	T (°C)	$\Delta\epsilon$	β_{cc}	log τ(s)	$\chi^2 \times 10^3$	MSEE $\times 10^3$
this study	151	1.41 ± 0.04	0.49 ± 0.01	−2.54 ± 0.04	0.58	6.02
this study	153	1.24 ± 0.03	0.55 ± 0.01	−3.08 ± 0.03	2.00	10.8
this study	154	1.09 ± 0.03	0.58 ± 0.02	−3.42 ± 0.03	2.93	13.1
ref 8	150	1.98 ± 0.15	0.45 ± 0.03	−2.55 ± 0.11	0.63	11.2
ref 8	152	1.42 ± 0.06	0.63 ± 0.03	−3.30 ± 0.04	1.82	19.1
ref 8	154	1.24 ± 0.07	0.64 ± 0.04	−3.90 ± 0.06	2.82	23.7
ref 8	156	1.34 ± 0.15	0.66 ± 0.09	−4.21 ± 0.10	15.6	55.8
ref 8	158	1.37 ± 0.07	0.63 ± 0.03	−4.66 ± 0.05	2.77	23.7
ref 8	160	1.21 ± 0.04	0.69 ± 0.02	−5.02 ± 0.02	0.82	12.8
ref 7	155	3.56 ± 3.17	0.36 ± 0.06	−1.80 ± 0.66	0.73	10.2
ref 7	158	2.21 ± 0.25	0.41 ± 0.02	−3.31 ± 0.17	0.48	8.25
ref 7	161	1.50 ± 0.06	0.52 ± 0.02	−4.46 ± 0.05	1.30	13.6
ref 7	164	1.31 ± 0.05	0.60 ± 0.03	−5.04 ± 0.04	2.58	19.2

(c) Havriliak–Negami Fits to PEEK Data

sample	T (°C)	$\Delta\epsilon$	α_{hn}	β_{hn}	log τ(s)	$\chi^2 \times 10^3$	MSEE $\times 10^3$
this study	151	1.21 ± 0.02	0.54 ± 0.04	0.73 ± 0.03	−2.27 ± 0.02	0.12	2.88
this study	153	1.19 ± 0.01	0.53 ± 0.03	0.73 ± 0.02	−2.65 ± 0.03	0.31	4.43
this study	154	1.09 ± 0.01	0.51 ± 0.04	0.75 ± 0.03	−2.94 ± 0.04	0.63	6.28
ref 8	150	1.96 ± 0.53	1.00 ± 0.75	0.46 ± 0.21	−2.56 ± 0.33	1.08	16.4
ref 8	152	1.41 ± 0.08	0.85 ± 0.37	0.67 ± 0.14	−3.21 ± 0.22	1.74	20.9
ref 8	154	1.25 ± 0.02	0.44 ± 0.04	0.84 ± 0.03	−3.36 ± 0.04	0.11	5.29
ref 8	156	1.45 ± 0.08	0.32 ± 0.07	1.00 ± 0.09	−3.56 ± 0.08	1.85	21.5
ref 8	158	1.54 ± 0.05	0.36 ± 0.06	0.86 ± 0.05	−3.99 ± 0.07	0.36	9.48
ref 8	160	1.45 ± 0.06	0.39 ± 0.06	0.82 ± 0.03	−4.47 ± 0.07	0.09	4.57
ref 7	155	3.02 ± 666	0.30 ± 33.9	1.00 ± 111	−1.70 ± 2.58	0.44	8.59
ref 7	158	1.26 ± 0.11	0.32 ± 0.07	1.00 ± 0.19	−3.47 ± 0.08	0.13	4.63
ref 7	161	1.37 ± 0.01	0.42 ± 0.02	0.82 ± 0.03	−3.99 ± 0.02	0.05	2.95
ref 7	164	1.34 ± 0.01	0.43 ± 0.01	0.82 ± 0.01	−4.49 ± 0.01	0.02	1.92

[a] χ^2 is the sum of squared residuals. MSEE is the model standard error of estimate.

symmetrical broadening parameters, β_{cc} and β_{fk}, are quite different, even though the plotted curve fits to data in Figure 4 appear, from visual inspection, to be very similar. In general, β_{cc} is larger than the corresponding value of β_{fk}.

HN Analysis. The fractional values of α_{hn} reflect the asymmetric broadening of the loss curves, and this is seen to be temperature independent for the three data sets considered, with the data recorded in this study being the least skewed. These data display the greatest extent of symmetrical broadening and, again, this shows very little dependence on temperature, whereas the relaxation strength decreases with increasing temperature. The relaxation strengths derived from the Kalika and Krishaswamy[8] and Huo and Cebe[7] data are similar in magnitude, yet neither shows a consistent decrease with increasing temperature. Through use of the HN function, the addition of an extra term to account for high-frequency skew has a significant impact on the magnitude and temperature dependence of the broadness and relaxation strength (compared with the FK and CC functions), which will, in turn, affect the numerical value of the RAP.

It is interesting to compare the temperature dependence of the α-relaxation for the three data sets as the isothermal temperatures are not totally coincident and the onset of PEEK crystallization, which is known to occur quite close to the DSC glass transition temperature of 143 °C, would be expected to influence the loss curve position. This can be done by plotting log τ_{hn}, determined from the HN analysis, against reciprocal temperature (Figure 5a). Disregarding the data point for Huo and Cebe[7] at 155 °C due to the inherent error, it is apparent that all three data sets exhibit similar temperature dependencies. The relaxation times for the data of Kalika and Krishnaswamy[8] are shifted to lower temperatures, however, such that, at an equivalent relaxation time there is a temperature discrepancy of about 4 °C with our data. The main feature of the relaxation time plots shown in Figure 5b is the divergence in log τ_{hn} from log τ_{fk} and log τ_{cc}, with increasing temperature.

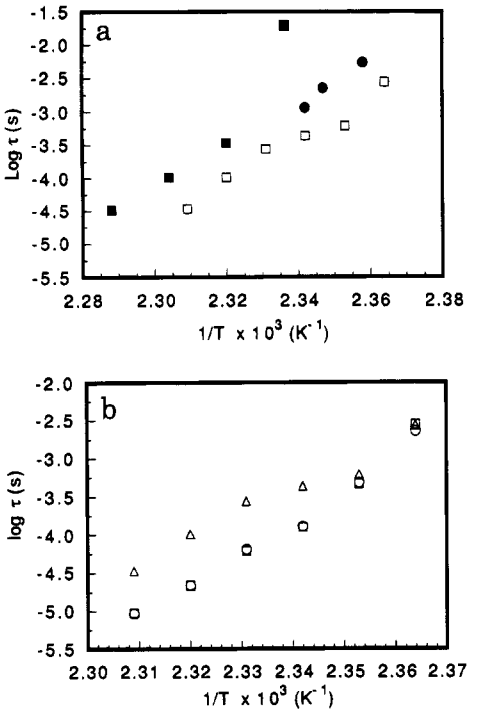

Figure 5. (a) log relaxation time against reciprocal temperature from Havriliak–Negami analysis of PEEK data: (○) this study; (□) ref 8; (■) ref 7. (b) log relaxation time against reciprocal temperature for PEEK data from ref 8: (○) Fuoss–Kirkwood analysis; (□) Cole–Cole analysis; (△) Havriliak–Negami analysis.

Discussion

Following these observations, a number of points can be made regarding the curve fitting of dielectric data and the use of isochronal and isothermal experimental methods to obtain such data. In order to fully characterize a loss process (at a particular temperature) and to minimize the curve-fitting errors when empirical functions are used, the loss curve peak and the high- and low-frequency tails need to fall within the available frequency window. The loss curve must be defined by the maximum number of data points that can be obtained. The most appropriate empirical equation should be employed to take account of features such as high-frequency skew which is commonly observed in the loss curves of amorphous polymers. Representing experimental data in the form of dielectric loss/frequency plots is preferable to the use of Cole–Cole plots since asymmetric broadening and the position of the loss maximum are more easily discerned in the former. Isothermal techniques offer a number of advantages over isochronal measurements. More data points can be obtained in a single isothermal frequency scan since, in an isochronal scan, limitations are imposed by the need to heat the sample at rates which restrict the number of frequencies that can be scanned. In this study, for example, the α-relaxation of PEEK has been characterized by up to 20 data points per temperature, compared with a maximum of 9 points from the converted isochronal scans. Furthermore, modern dielectric bridges can scan wide-frequency ranges in less than 1 min. The data from an isochronal scan also require further manipulation to convert it to an isothermal form suitable for curve fitting. Using isothermal techniques, the sample can be removed after every frequency sweep for characterization and examination, whereas isochronal scans can be affected by dynamic crystallization of the sample during heating. Changes in sample morphology during an isochronal scan cannot be easily monitored in situ and are difficult to determine after the experiment if a wide temperature range has been covered. This is important when monitoring the dielectric response of polymers, in the amorphous state, which rapidly crystallize above the glass transition. Our analysis has shown that values of the relaxation strength for the α-relaxation of PEEK are dependent upon the particular empirical function used. This suggests, therefore, that use of an inappropriate function in data fitting is likely to lead to an inaccurate estimation of the magnitude of the RAP in semicrystalline polymers.

References and Notes

(1) Cogswell, F. N. *Thermoplastic Aromatic Polymer Composites*; Butterworth-Heinemann: Oxford, U.K., 1992.
(2) Grebowicz, J.; Lau, S. F.; Wunderlich, B. *J. Polym. Sci., Polym. Symp.* **1984**, *71*, 19.
(3) Suzuki, H.; Grebowicz, J.; Wunderlich, B. *Makromol. Chem.* **1985**, *186*, 1109.
(4) Suzuki, H.; Wunderlich, B. *Br. Polym. J.* **1985**, *17*, 1.
(5) Cheng, S. Z. D.; Cao, M. Y.; Wunderlich, B. *Macromolecules* **1986**, *19*, 1868.
(6) Krishnaswamy, R. K.; Kalika, D. S. *Polymer* **1994**, *35*, 1157.
(7) Hou, P.; Cebe, P. *Macromolecules* **1992**, *25*, 902.
(8) Kalika, D. S.; Krishnaswamy, R. K. *Macromolecules* **1993**, *26*, 4252.
(9) Draper, N. R.; Smith, H. *Applied Regression Analysis*, 2nd ed.; Wiley: New York, pp 28–31.
(10) Fuoss, R. M.; Kirkwood, J. *J. Am. Chem. Soc.* **1941**, *63*, 385.
(11) Cole, R. H.; Cole, K. S. *J. Chem. Phys.* **1941**, *9*, 341.
(12) Havriliak, S.; Negami, S. *Polymer* **1967**, *8*, 161.

MA950217R